# International Journal of Mechanical Engineering and Technology (IJMET)

Volume 14, Issue 06, Nov-Dec 2023, pp. 23-36. Article ID: IJMET\_14\_06\_004 Available online at https://iaeme.com/Home/issue/IJMET?Volume=14&Issue=6 ISSN Print: 0976-6340 and ISSN Online: 0976-6359

Impact Factor (2024): 20.99 (Based on Google Scholar Citation)





# NOVEL DESIGNS FOR EJECTOR-BASED SYSTEMS FOR ENHANCED FLUID RECOVERY VERIFIED THROUGH CFD SIMULATIONS

#### Nithin S. Panicker\*

Oak Ridge National Laboratory, Nuclear Energy and Fuel Cycle Division, 1 Bethel Valley Road, Oak Ridge, Tennessee 37830, USA Corresponding Author

#### **Gaurav Bazaz**

Spar Systems Inc., Montvale, New Jersey 07645, USA

#### Vivek M. Rao

Oak Ridge National Laboratory, Nuclear Energy and Fuel Cycle Division, 1 Bethel Valley Road, Oak Ridge, Tennessee 37830, USA

#### **Shashank Natesh**

Spar Systems Inc., Montvale, New Jersey 07645, USA

#### Prashant K. Jain

Oak Ridge National Laboratory, Nuclear Energy and Fuel Cycle Division, 1 Bethel Valley Road, Oak Ridge, Tennessee 37830, USA

#### **ABSTRACT**

Ejector-based systems are widely used for various industrial purposes, including transporting fluids, trapping particulate matters, and refrigeration. Novel design strategies can aid in the enhancement of key performance parameters such as entrainment ratio (ER) and entrained mass flow rate, resulting in an increase in energy efficiency over conventional designs. This study included analysis of two novel design features that can increase both ER and the entrained mass flow rate: repeated entrainment and the wrapped multi-nozzle. Computational fluid dynamics (CFD) simulations were performed to verify the enhanced performance offered by these designs. The ER predicted by the CFD model for a downscaled design of the repeated entrainment is validated using the data acquired through in-house experiments. CFD predictions for ER and entrained mass flow rates for three different inlet pressures are reported for both designs. The repeated entrainment design provides nearly 50 times more ER than the wrapped multi-nozzle. However, the wrapped multi-nozzle design provides 3 times more fluid recovery/mass flow rate than the repeated entrainment design.

**Keywords:** Computational Fluid Dynamics (CFD), Designs, Ejectors, Refrigeration

Cite this Article: Nithin S. Panicker, Gaurav Bazaz, Vivek M. Rao, Shashank Natesh and Prashant K. Jain, Novel Designs for Ejector-Based Systems for Enhanced Fluid Recovery Verified Through CFD Simulations, International Journal of Mechanical Engineering and Technology (IJMET), 14(6), 2023, pp. 23-36. https://iaeme.com/Home/issue/IJMET?Volume=14&Issue=6

# 1. INTRODUCTION

Ejectors have many industrial applications and are widely used for conveying fluids, management of hydrogen recirculation in fuel cells [1], evacuation of corrosive fumes in chemical industries, refrigeration [2], and trapping micrometer-sized particulate matters (venturi scrubbers). The ejector's wide applicability can be attributed to its simplicity in construction, lack of moving parts, along with its ability to reduce throttling losses [3], [2]. The main objective of this study is to introduce design concepts that enhance the performance of the ejector-based systems by improving entrainment ratio (ER) and secondary flow mass recovery. An ejector is a system (**Fig. 1**) in which high-pressure motive fluid passes through a conical motive fluid nozzle. The motive fluid nozzle converts the high pressure of the flow into kinetic energy. Because of the negative pressure (subatmospheric) generated from the venturi effect, the motive fluid entrains the fluid from the secondary inlet (typically connected to a source), and the fluid mixture (motive-entrained) exits through the outlet.

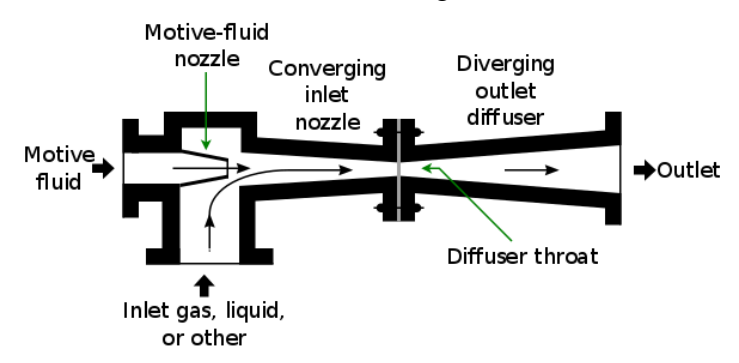


Fig. 1 Schematic of a conventional ejector (CC BY

https://commons.wikimedia.org/wiki/File:Ejector\_or\_Injector.svg)

ER is a key parameter that determines the performance of an ejector [4], [1], [2] and can be determined using the formula below:

$$ER = \frac{\text{Mass flow through entrainment}}{\text{Primary motive mass flow}}$$

Ejectors can be operated with various primary-secondary fluid combinations: gas-gas, gas-liquid, or liquid-liquid. The subsequent discussion addresses gas-gas ejectors operating in the subsonic mode unless otherwise stated explicitly. This work proposes innovative design variations from the traditional ejector design for ejectors operating in subsonic regime, with air as primary and secondary fluids. There are many published materials on ejectors, especially for refrigeration cycle [2] and CFD-based performance investigation of ejectors [5,6,7]. Because the current work is focused on novel designs based primarily on motive nozzles and entrainment ducts of an ejector-type system, the subsequent literature review will be exploring the design concepts present in the literature relevant to ejector-components, in particular, motive nozzles and entrainment ducts, and the associated performance improvement.

# 2. A REVIEW OF DIFFERENT DESIGNS OF EJECTORS AND THEIR EFFECT ON PERFORMANCE

Chang and Chen [8] conducted experiments to evaluate the performance of a petal-shaped motive nozzle for an ejector over a traditional conical motive nozzle used for ejector-based refrigeration cycle in which ER and energy efficiency were observed. They found that the coefficient of performance of a petal-shaped nozzle was superior to that of the conical nozzle for area ratios (i.e., mixing chamber cross-section / motive nozzle outlet) greater than 180. Maqsood [9] performed an experimental investigation of bent ejectors with oblong mixing chamber. The bent section decreased the ER because of the reduction in flow area caused by recirculation around the bend. The temperature ratio between the secondary and the primary flow had a significant effect on the pumping ratio. Temperature had a negligible effect, if any, on the pressure drop across an ejector. The high viscosity and turbulence kinetic energy of the hot primary flow improves the mixing of primary and secondary flows and reduces the separation, therefore improving ER. However, the efficiency of the hot flow cases is lower than that of the cold flow cases because the driving force (i.e., the inlet dynamic pressure) of the hot flow is much higher than that of a comparable cold flow case. Meakhail et al. [10] performed an experimental investigation on ejectors used for refrigeration cycle to understand performance, with the variation in motive nozzle numbers placed axisymmetrically, with internozzle spacings, with mixed chamber lengths, and at different diffuser angles. The variation in efficiency with respect to the number of nozzles was negligible, and the ideal inter-nozzle spacing is the diameter of the nozzle throat. Furthermore, the ejector efficiency increased by 1% when the diffuser angle was 14 degrees. Li et al. [11] conducted a performance investigation of both gas-liquid and gas-gas ejectors by carrying out computational fluid dynamics (CFD) simulations. They used various working fluids (primary/secondary) by adjusting the mixing chamber length and primary nozzle position. The combination of helium (primary fluid) and liquid oxygen (secondary fluid) provided the maximum ER up to 200. The combination of gas and gas as the working fluid always produced low entrainment compared to gas and liquid. An optimum length of the mixing chamber was determined to provide maximum ER. Additionally, the effect of primary nozzle placement was dependent on this length to achieve maximum ER. Using an experimentally validated CFD and analytic model, Alimohammadi et al. [12] investigated the performance of a supersonic ejector used as a compressor for the vehicle cooling refrigeration cycle powered by the hot water inside the radiator. It was concluded that the ER increased with the reduction in the throat diameter of the primary nozzle. Moreover, the increased diffuser exit diameter yielded lower ER. Increasing the mixing chamber diameter caused reverse flow and therefore lowered ER, whereas reducing the diameter to a very low value also reduced ER. Therefore, it can be concluded that an optimum mixing chamber diameter is required for optimum ER. The length of the mixing chamber and diffuser had a minimal effect on ER. Ramesh and Sekhar [13] studied the effect of the suction chamber angle on the ER. It was inferred that ER increased when the suction chamber angle increased from 0 to 12 degrees, and further increment reduced the ER. It was concluded that although there was change in ER, the change is highly dependent upon the operating condition. Rogie et al. [14] developed a simple 1D model of an ejector to optimize the fueling process of hydrogen-based vehicles. ERs up to 15 were observed in their model, with ER decreasing with an increase in back pressure or the fuel tank pressure. Finally, a fueling procedure was simulated to compare the conventional valve system with the ejector system's pressure tank at the optimum area ratio. The simulation results in a 6% faster fueling time compared to that obtained using a traditional expansion valve. It was concluded that the use of ejectors for fueling hydrogen vehicles could result in savings associated with the reduction of high-pressurized hydrogen usage.

Mensik [15] performed an experimental investigation of ER by offsetting the motive nozzle with the central axis of symmetry of the ejector. There was a loss of 12% ER when the nozzle was offset. Therefore, application of the concept of offsetting did not yield any benefits.

In this work, a repeated entrainment concept using multiple entrainment ducts in serial and a multiple nozzle concept arranged in a zig-zag fashion is introduced, and its effect on the ER and the entrainment mass flow rate is analyzed. Based on the literature review and experiments conducted in this work, the novel designs proposed in this work could improve the performance of ejector-based systems in venturi scrubbers, hydrogen fueling, refrigeration, and many others. The ER and entrainment flow rates achieved by these designs are verified using CFD simulations. The remainder of the sections are arranged as follows: (1) CFD modeling and simulation setup, in which the CFD model and its description are provided; (2) validation, in which the model prediction of the ER is compared with experiments; (3) results and discussion; and (4) conclusion.

# 3. CFD MODELING AND SIMULATION SETUP

Flow is subsonic and assumed to be incompressible. A steady state Reynolds-averaged Navier—Stokes (RANS) model with the realizable k-epsilon model to account for turbulence is used in most CFD-based studies of ejectors [5,6,7]. Therefore, a similar modeling approach is followed in this study using commercial CFD software StarCCM+. A polyhedral mesher is used to discretize the computational volume of every geometry studied because of its ability to resolve the complex curvatures with minimal meshing effort. Air viscosity of 1.8E-5 Pa-s and density of 1.2 kg/m³ are used for the simulation. All Y+ wall treatment models available within StarCCM+ are used to provide accurate predictions agnostic to wall Y+, relaxing the stringent mesh requirement for the first computational cell above the wall boundary to match a particular wall Y+ value—usually <1 or >30. Fixed gauge pressure is applied to the inlet boundary of the motive nozzle in the range of 2,000 Pa-16,000 Pa, and 0 Pa gauge (atmospheric pressure) is applied on the inlets of the entrainment ducts.

#### 4. VALIDATION OF CFD MODEL WITH EXPERIMENTAL STUDY

The geometry of the design used for validation was 3D printed using selective laser sintering with PA12 polymer material (Fig. 2). The entrainment duct was printed in two major parts which were joined on flanges. Additionally, support structures were added to hold the system intact. An adapter was designed to connect the inlet of the motive nozzle to the outlet of the blower. This adapter was also 3D printed using the same process and materials. A moderately powered Tobargar inflatable blower (450 W) was used to generate the motive flow which drives the entrainment process. The blower supplies air at a gauge pressure of about 1,650 Pa. When the blower is switched on, the air from the blower passes through the inlet of the motive nozzle. The air accelerates through the convergent and constant area throat section of the nozzle and emerges as a high-speed jet on the outlet of the throat. As the jet passes through the entrainment inlets, it creates negative pressure, which sucks or entrains the stationary ambient air through the entrainment inlets. This entrained air then joins the motive jet and exits from the main outlet. Air flow was measured using a Testo 405i hot wire anemometer which provides velocity measurements with high sensitivity in small spaces. Velocity measurements were made at the jet and the outlet (Fig. 3) at evenly distributed sets of points. These measurements give the local flow velocity, and averaging of the individual velocities gives the local area velocity. This local area velocity is multiplied by the local area to obtain the flow rate. The trials were repeated at least 10 times to gain sufficient confidence in the measurement of the outlet flow rate, thus providing the ER.

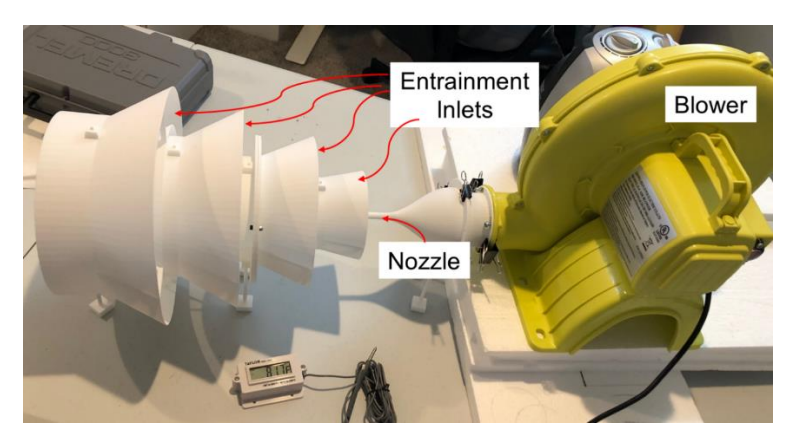


Fig. 2 Entrainment duct with single tube motive nozzle used in experiment

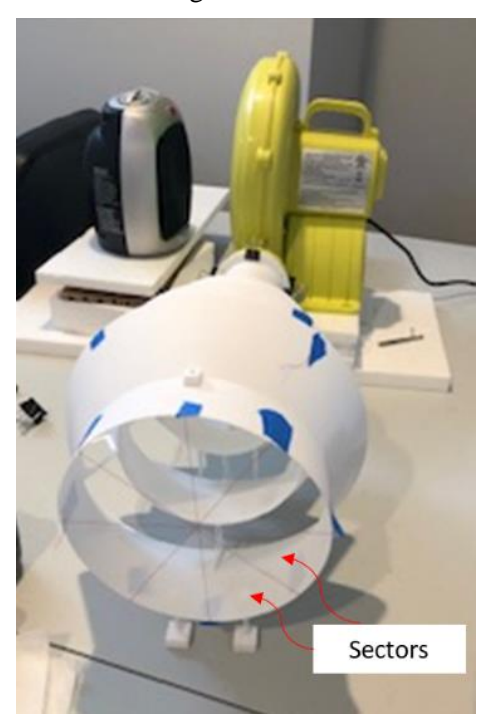


Fig. 3 Sectors considered for flowrate measurement

# 5. COMPARISON OF CFD PREDICTION OF ER WITH EXPERIMENTAL DATA

Flow is assumed to be symmetric because of the symmetry of the overall geometry and the motive jet emerging from the nozzle in Fig. 2. Therefore, only a quarter portion of the geometry is used for the simulation and validation to save computational cost. A polyhedral masher in StarCCM+ is used to generate the mesh for CFD calculations. Six prism layers were generated on the wall boundaries (see Fig. 4) of the motive nozzle and entrainment ducts to capture the boundary layer of the motive and entrained flow, respectively.

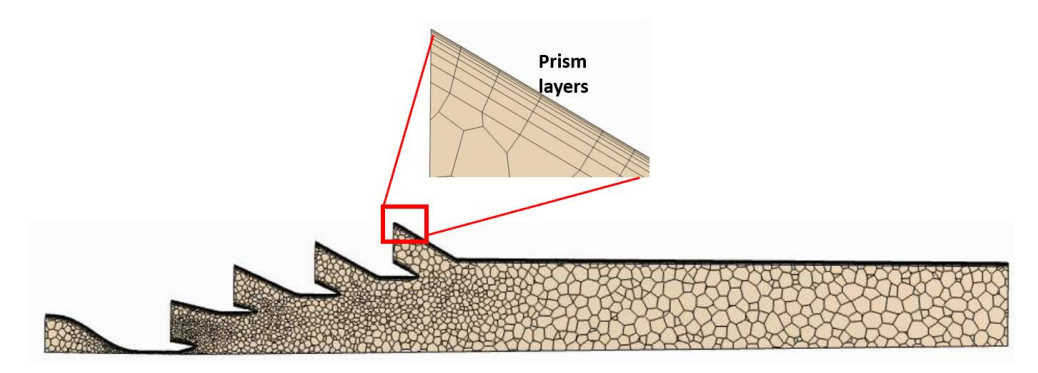


Fig. 4 Mesh on a cross section of the geometry

Gauge pressures of 1,650 Pa and -5 Pa (Table 1) were applied on the inlet and outlet boundary of the geometry, respectively, and a pressure of 0 Pa was applied at the entrainment duct inlets. Entrainment ratio predicted by the simulation and measured by the experiment is shown in Table 2.

**Table 1** Boundary pressures used for simulation from the experiment

Boundary	Gauge pressure (Pa)
Inlet	1,650
Outlet	-5
Entrainment inlet	0

Table 2 Entrainment ratio CFD vs. experiment

	Entrainment ratio
Experiment	60
Simulation	53
Error	11%

An error of 11% is observed between the measurement and the CFD prediction. This error can be attributed to the uncertainty in the gauge pressure measurement at the outlet or the flow-averaged RANS approach followed for modeling. A true direct numerical simulation or a large eddy simulation model that can precisely resolve the wall boundary layer could improve the prediction to match the experimental measurement. However, the simulation requires a substantially higher computational cost which is beyond the scope of this work. This error is acceptable because this study is conducted to estimate the ER rather than to determine a value with highest accuracy to prove that the proposed designs are showing a high value of ER, or a higher value of suction mass flow rate compared to traditional designs seen in the literature. The model validated here is deployed for all the simulations described in the subsequent sections.

# 6. RESULTS AND DISCUSSION

#### **6.1. Repeated entrainment**

Geometries in

Fig. 5 are used to achieve repeated entrainment. It consists of a motive nozzle and entrainment duct/ducts. The motive nozzle is made of a conical section followed by an ultrathin tube 5 mm in diameter. The tube is attached to an entrainment duct, which is a conical section with an inlet to entrain air. The conical section is connected to a cylindrical channel through which the mixture of the jet from motive nozzle and the entrained jet exits the system through its outlet.

Multiple entrainment ducts are arranged in serial to enclose the outlets of each former duct and are used to repeatedly entrain air through the inlets using a single motive jet.

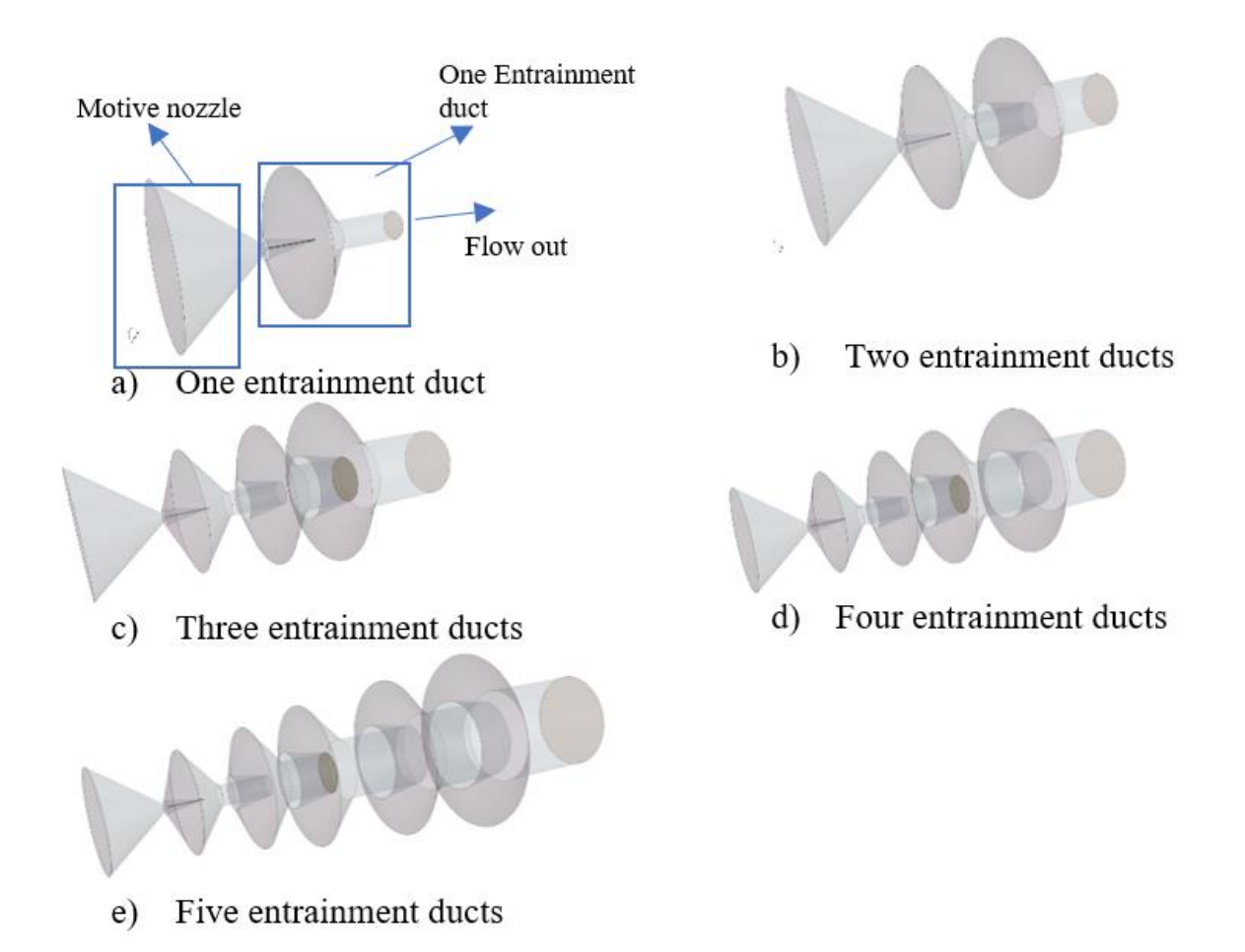


Fig. 5 Designs to achieve repeated entrainment with multiple entrainment ducts.

Most designs [3], [18], [13], [8] for ejector-type systems use a single entrainment duct with a single inlet to entrain secondary fluid using the primary or motive fluid. Fig. 6 shows the velocity contour on a plane passing through the axis. The motive jet, which is generated by the static pressure applied on the inlet of the motive nozzle, passes through the multiple entrainment ducts. The atmospheric air at a higher pressure than the surface of the motive jet entrains through the inlet of the first entrainment duct, and the combination of motive and entrained jets from the first duct enters the second duct and generates low pressure in the second duct, ensuing further entrainment. This process repeats across the entire length of the geometry providing substantially high ER and entrained mass recovery over traditional design with just one conical motive nozzle and a duct.

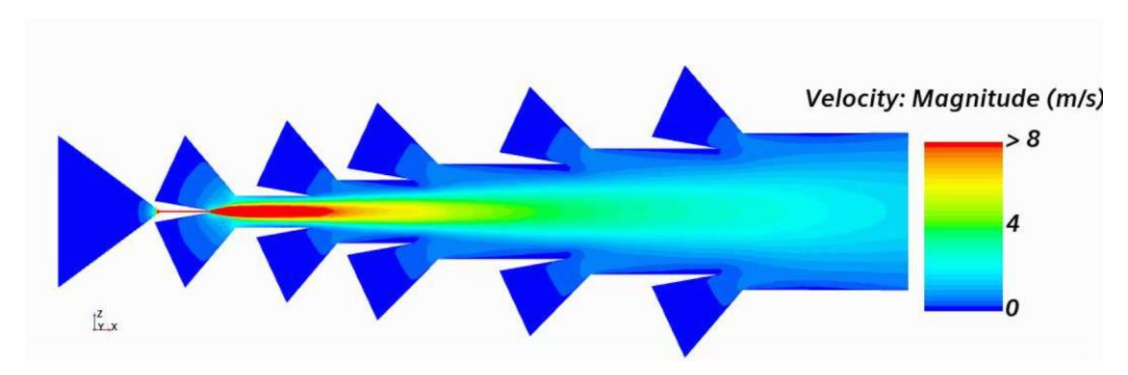


Fig. 6 Velocity contour on a cross-section of repeated entrainment design with five entrainment ducts

Turbulent kinetic energy on a cut-plane is shown in Fig. 7. Peak turbulence is observed in the bulk of the integrated duct, after the outlet of the first duct. The turbulence is caused by the interaction between the motive jet and succesively entrained jets, and it intensifies progressively as the mixture of motive and entrained jets passes through the duct because of the cumulative effect of the turbulence upstream. Turbulent dissipation is proportional to the turbulent kinetic energy for RANS models. Therefore, the profile of turbulent dissipation inside the duct will be similar to the turbulent kinetic energy and is not reported.

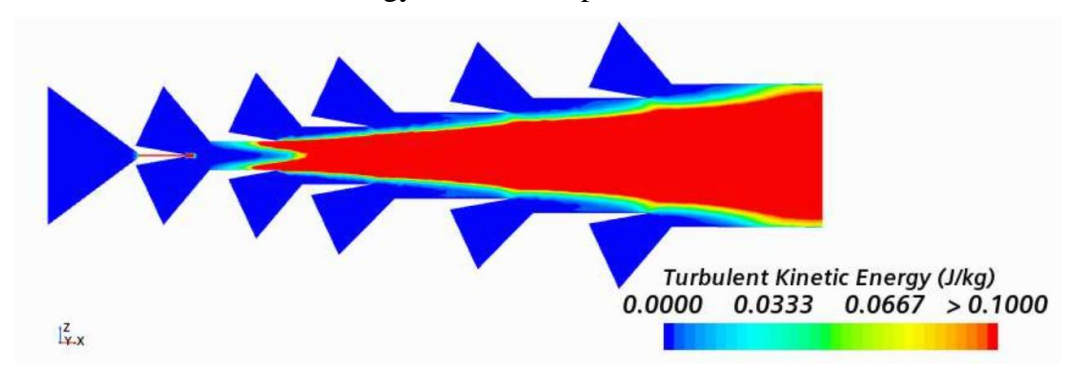


Fig. 7 Turbulent kinetic energy profile

The variation of ER with increase in the number of entrainment ducts and for different inlet pressures is provided in Fig. 8. As expected, the ER increases with the number of ducts; however, it is interesting to note that the increase in ER is nonlinear and increases at a higher rate for repeated entrainment . The entraiment ratio is nearly invariant with pressure, suggesting that minimal gain can be achieved by increasing the pressure.

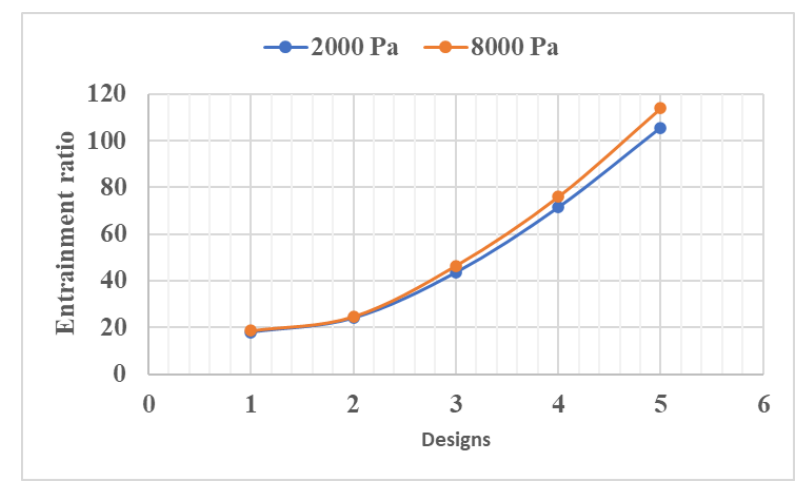


Fig. 8 Entrainment ratio vs. designs for different inlet pressures for repeated entrainment concept

The entrained mass flow rate and the motive fluid flow rate (with an increase in the number of entrainment ducts for inlet pressure  $= 8,000 \, \text{Pa}$ ) are shown in Fig. 9. The motive flow rate is nearly constant, whereas the entrained flow rate increases nonlinearly, which is expected because of its dependence on ER. However, it is interesting to note that if the pumping power = pressure drop  $\times$  motive flow rate for nearly the same motive fluid pumping cost, increasingly larger entrained fluid flow rates can be achieved with the serial addition of entrainment ducts.

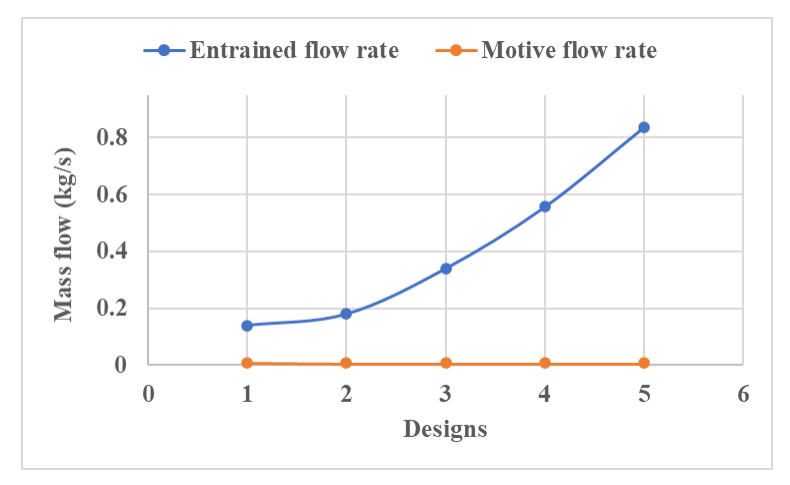


Fig. 9 Entrained flow rate vs. designs for different inlet pressures for repeated entrainment concept

This concludes the discussion of the hypothesis that the repeated entrainment design concept can substantially increase ER and has the potential to provide superior entrained mass flow rate at a lower motive flow pumping cost over that of traditional designs.

# 8. WRAPPED MULTI-MOTIVE NOZZLE DESIGN

The geometry of the the wrapped design shown in Fig. 10 is a combination of a motive nozzle and an entrainment duct. The motive nozzle (in yellow) consists of a small array of tubes arranged in a zig-zag pattern on a rectangular panel and a convergent nozzle connected to the rectangular panel for motive flow enterance to the tubes and ejection through outlets of the tubes into the entrainment duct/chamber. The entrainment duct is a convergent nozzle (in orange) enclosing the motive nozzle. The secondary fluid, which is air for this study, enters through the inlet of the entrainment duct because of suction. The convegent nozzle of the entrainment duct is connected to an outlet channel through which both the entrained and motive jet exit. The convegent nozzles of the motive nozzle and the entrainment duct are streamlined to reduce flow resistance and maximize flow rate for a given inlet pressure. Multiple tubes used in the motive nozzle provide higher motive jet flow rates compared to a single tube for the same inlet pressure, therefore resulting in higher entrainment flow rates. Additionally, a zig-zag arrangement is used to promote contact between the entrained jet and the motive jet through the triangular gaps between two sets to increase the entrainment or suction.

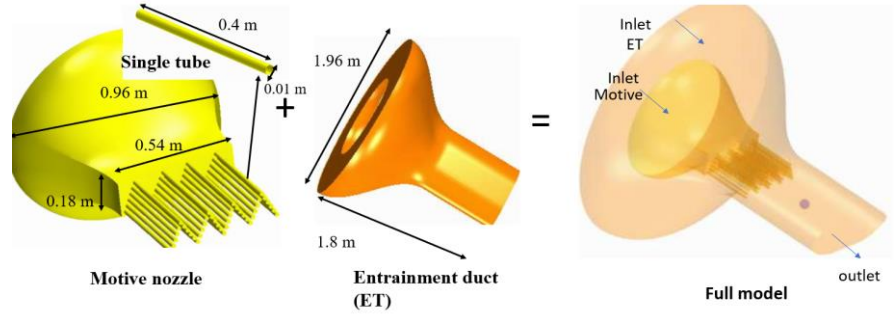


Fig. 10 Geometry of wrapped multi-nozzle design

The air's static pressure in the convergent section of the motive nozzle is converted to kinetic energy at the tubes, resulting in a high velocity jet which enters the entrainment duct, as seen in Fig. 11 (a). This generates low pressure or vacuum in the entrainment duct, as shown in Fig. 11 (b). The vacuum generated within the duct sucks air through the entrainment inlet into the duct and the motive and entrained jet mixes and then exits through the outlet. Flow separations are observed on both sides of the outlet channel close to the exit, thus blocking the incoming entrained jet through the entrainment inlet. The prevention of this flow separation through innovative design methods can further enhance the ER and the entrained flow rate, which will be analyzed in future work. Turbulent kinetic energy (TKE) profile is moderately exaggerated for effective visualization as shown in Fig. 11 (c); the highest TKE is observed near the walls of the outlet channel and the spaces between the nozzle tubes. Higher turbulence near the side walls of the outlet channel is attributed to the flow separation and the turbulent mixing of motive and entrained jet interfaces in those regions. The turbulent energy peaks near the tubes are because of the interaction of entrained jet with the outer tube walls.

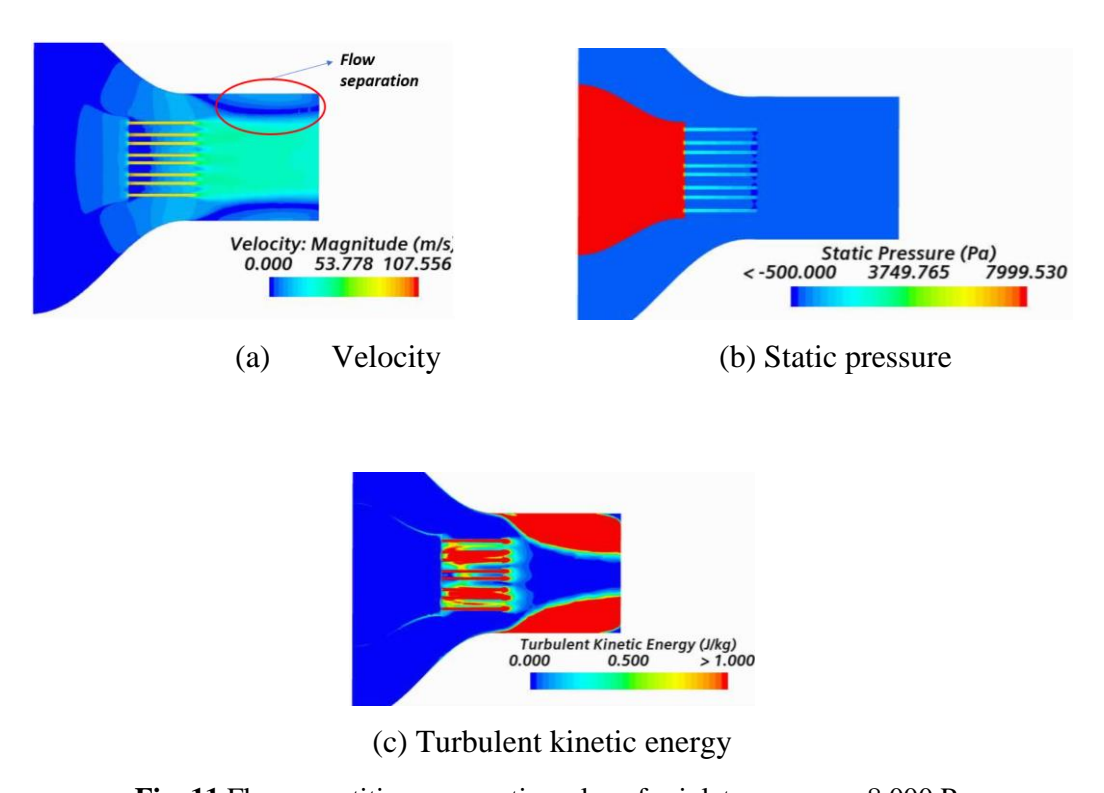
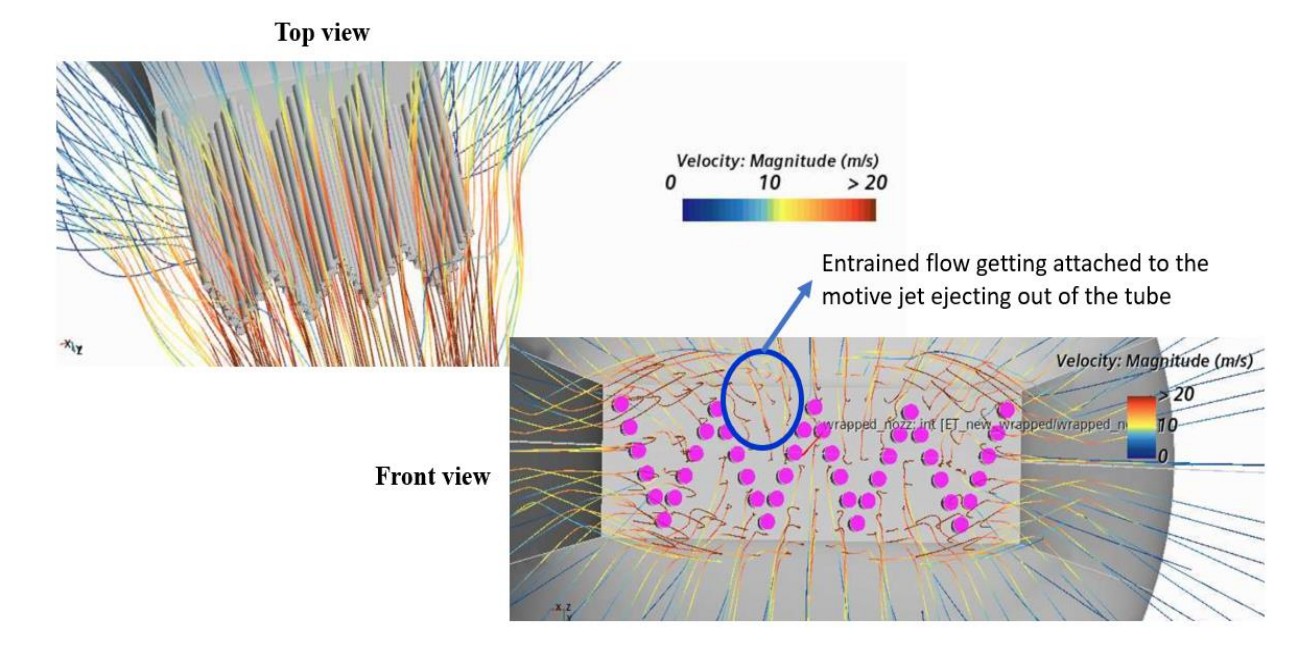


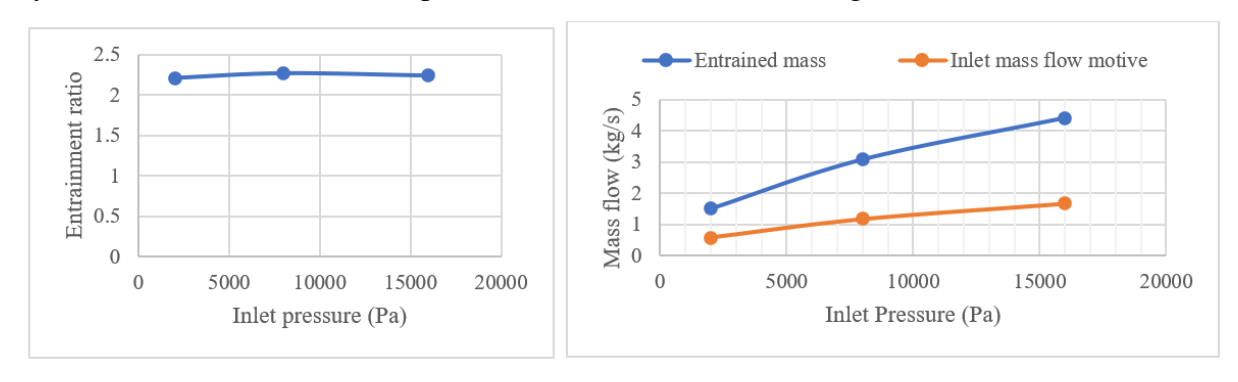
Fig. 11 Flow quantities on a section-plane for inlet pressure = 8,000 Pa

The streamlines of entrained air passing between the sets of tubes are shown in Fig. 12. It can be inferred from the plot that there is a significant entrainment induced between the tube sets, validating the theory that entrainment is enhanced by increasing the area of contact between the entrainment jet and the motive jet compared to the geometry of conventional single conical motive nozzle models.



**Fig. 12** Entrained flow velocity streamline around the motive nozzle tubes (pink) in the entrainment chamber

The ER achieved through this design for three different pressures—2,000 Pa, 8,000 Pa, and 16,000 Pa—is shown in Fig. 13 (a). As observed for the repeated entrainment case, the ER does not vary with inlet pressure: it is geometry-dependent, and it reaches a constant value of ~2.2. The ER for repeated entrainment is substantially higher than the ER for the wrapped multimotive. However, for the repeated entrainment case, the mass flow rate achieved was small, even after adding five entrainment ducts which resulted in excessive system size. The wrapped design, which is much smaller in size, provides nearly three times the mass flow rates provided by five ducts for the same inlet pressure = 8,000 Pa, as seen in Fig. 13 (b).



(a) ) ER vs. inlet pressure,

(b) mass flow rate vs. inlet pressure

Fig. 13 Wrapped multi-motive-nozzle performance

The increase in inlet pressure increases motive mass flow rates, which entrains more air and increases the entrainment mass flow rates. It is believed that an annular motive nozzle configuration [4] and a petal motive nozzle concept [8] are the only designs of motive nozzle reported in the literature that are deviant from the traditional conical single motive nozzle used in typical ejectors. The ER reported for the annular nozzle configuration is below 1 and is inferior to the wrapped nozzle design discussed herein. Although the ER achieved for the petal nozzle is comparable to the wrapped nozzle design presented in the current study, the entrained mass flow rate is not reported in the literature and therefore is not available for comparison with the wrapped nozzle design results.

Based on the high inlet motive pressures (>100 kPa) used in their study [5], it can be deduced that a significantly higher energy is spent by the petal design to achieve the same ER as the wrapped nozzle design, which uses approximately ½0 of inlet pressure used for petal nozzle to drive the motive jet. It is also difficult to arrive at a firm conclusion on the superiority of these nozzle designs because of different modes of operation: the petal nozzle's flow is supersonic, whereas the wrapped motive nozzle's flow is subsonic. Therefore, in future work, inlet pressure of the motive nozzle will be elevated to create supersonic flow in the entrainment duct, and the resulting ER will be investigated.

#### 7. CONCLUSION

Ejector-based systems are widely used for various industrial purposes, and the performance improvement of such systems would be immensely beneficial. ER and entrained mass flow rate of fluid are key parameters that affect the energy efficiency of these systems. In the current study, two novel designs are proposed to substantially increase the ER and entrained mass flow rate over the conventional single conical nozzle and duct designs: repeated entrainment and the wrapped multi-nozzle.

# 7.1. Repeated entrainment

In the repeated entrainment design, multiple entrainment ducts follow the motive nozzle to reuse the energy of the single motive jet exiting the motive nozzle to entrain fluid successively. An ER up to 100 was achieved using five entrainment ducts, and there is a potential to achieve even higher ERs with the use of more than five entrainment ducts. Moreover, the entrained fluid recovery or mass flow rates can be increased significantly with a lower motive jet pumping cost compared to that of traditional designs, thus enabling energy efficient fluid transport. For the design analyzed herein, ER did not vary significantly with inlet pressure.

# 7.2. Wrapped multi-nozzle

The wrapped multi-nozzle design has multiple motive nozzles arranged in a zig-zag pattern to increase the motive flow rates for the same inlet pressure as that used in the repeated entrainment to achieve high entrained mass flow rates. The zig-zag arrangement was used to increase the contact area between the motive jet and the entrained jet to achieve high entrained fluid recovery. The entrainment ratio remained at nearly 2 with the change in inlet pressure. However, the mass flow rates ranged up to 4.2 kg/s, for an inlet pressure of 16 kPa. Although ER is lower for this design compared to repeated entrainment, the mass flow rate achieved was 3 times more than repeated entrainment for almost ½ of the system size.

These designs successfully demonstrate the capability of handling fluids in ejector-based systems with better control and energy efficiency than traditional ejector designs.

## **ACKNOWLEDGEMENTS**

The authors are grateful for the funding support provided by Department of Energy's High Performance Computing for Energy Innovation grant for this work.

# **Availability of Data and Materials**

The authors declare that the data supporting the findings in the manuscript is available up on request.

#### **Funding**

This work was funded by Department of Energy's High-Performance Computing for Energy Innovation grant.

## **Competing interests**

There are no financial or non-financial competing interests.

#### REFERENCE

- [1] Zhu, Y., Li Y., and Cai W. Control oriented modeling of ejector in anode gas recirculation solid oxygen fuel cell systems [Journal]. [s.l.]: Energy Conversion and Management, 2011. 4: Vol. 52.
- [2] Besagni, G., Mereu, R., and Inzoli, F. Ejector refrigeration: A comprehensive review [Journal]. [s.l.]: Renewable and Sustainable Energy Reviews, 2016. Vol. 53.
- [3] Kornhauser, A. A. The use of an ejector as a refrigerant expander [Book]. 1990.
- [4] Milewski J., Miller, A., and Salacinski, J. Off-design analysis of SOFC hybrid system [Journal]. [s.l.]: International Journal of Hydrogen Energy, 2007. 6: Vol. 32.
- [5] Pianthong K., Seehanam, W., Behnia, M., Sriveerakul, T., and Aphornratana, S.Investigation and improvement of ejector refrigeration system using computational fluid dynamics technique [Journal]. [s.l.]: Energy Conversion and Management, 2007. 9: Vol. 48.
- [6] De Oliveira Marum, V.J., Reis, L.B., Maffei, F.S., Ranjbarzadeh, S., Korkischko, I., dos Santos Gioria, R., and Meneghini, J. R. Performance analysis of a water ejector using Computational Fluid Dynamics (CFD) simulations and mathematical modeling [Journal]. [s.l.]: Energy, 2021. Vol. 200.
- [7] Han Y., Wang, X., Sun, H., Zhang, G., Guo, L., and Tu, J. (2019) CFD simulation on the boundary layer separation in the steam ejector and its influence on the pumping performance [Journal]. [s.l.]: Energy, 2019, Vol. 167.
- [8] Chang, Y. J., and Chen, Y. M. Enhancement of a steam-jet refrigerator using a novel application of the petal nozzle [Journal]. [s.l.]: Experimental Thermal and Fluid Science, 2000. 3-4: Vol. 22.
- [9] Maqsood, A. A study of subsonic air-air ejectors with short bent mixing tubes [Report]. [s.l.]: Queen's University, 2008.
- [10] Meakhail, T. A. et al. Experimental study of the effect of some geometric variables and number of nozzles on the performance of a subsonic air—Air ejector [Journal]. [s.l.]: Proceedings of the Institution of Mechanical Engineers, Part A: Journal of Power and Energy, 2008. 8: Vol. 222.
- [11] Li, C., Li, Y., and Wang L. Configuration dependence and optimization of the entrainment performance for gas—gas and gas—liquid ejectors [Journal]. [s.l.]: Applied Thermal Engineering, 2012. Vol. 48.
- [12] Alimohammadi, S., et al. A validated numerical-experimental design methodology for a movable supersonic ejector compressor for waste-heat recovery [Journal]. [s.l.]: Journal of Thermal Science and Engineering Applications, 2014. 2: Vol. 6.
- [13] Ramesh, A. S., and Sekhar, J. S. Experimental studies on the effect of suction chamber angle on the entrainment of passive fluid in a steam ejector [Journal]. [s.l.]: Journal of Fluids Engineering, 2018. 1: Vol. 140.
- [14] Rogie B., et al. Numerical optimization of a novel gas-gas ejector for fuelling of hydrogen vehicles. International journal of hydrogen energy [Journal]. [s.l.]: International journal of hydrogen energy, 2020. 41: Vol. 45.
- [15] Mensik, R. M. Characterization of the Effects of Jet Radial Position on Entrainment Ratio in a Subsonic Ejector [Report]. [s.l.]: Master thesis, Schulich School of Engineering, 2022.
- [16] Sriveerakal, T., Aphornratana, S., and Chunnanond, K. Performance prediction of steam ejector using computational fluid dynamics: Part 1. Validation of the CFD results [Journal]. [s.l.]: International Journal of Thermal Sciences, 2007. 8: Vol. 46.
- [17] Kong, F., and Kim, H. D. Optimization study of a two-stage ejector–diffuser system [Journal]. [s.l.]: International Journal of Heat and Mass Transfer, 2016. Vol. 101.

- [18] Sharifi, N., and Sharifi, M. Reducing energy consumption of a steam ejector through experimental optimization of the nozzle geometry [Journal]. [s.l.]: Energy, 2014. 860-867: Vol. 66.
- [19] Annual Energy Outlook 2023. https://www.eia.gov/tools/faqs/faq.php?id=1174&t=1 [Conference]. 2023.
- [20] Ejector CC-BY (https://commons.wikimedia.org/wiki/File:Ejector\_or\_Injector.svg). [wiki link].
- [21] Sampedro, E. O. Variable Entrained Flow Ejector. In 18th International Refrigeration and Air Conditioning [conference]. [s.l.]: Conference at Purdue, 2021.

#### \*Corresponding author email: panickerns@ornl.gov

This manuscript has been authored by UT-Battelle, LLC, under contract DE-AC05-00OR22725 with the US Department of Energy (DOE). The US government retains and the publisher, by accepting the article for publication, acknowledges that the US government retains a nonexclusive, paid-up, irrevocable, worldwide license to publish or reproduce the published form of this manuscript, or allow others to do so, for US government purposes. DOE will provide public access to these results of federally sponsored research in accordance with the DOE Public Access Plan (http://energy.gov/downloads/doe-public-access-plan).

**Citation:** Nithin S. Panicker, Gaurav Bazaz, Vivek M. Rao, Shashank Natesh and Prashant K. Jain, Novel Designs for Ejector-Based Systems for Enhanced Fluid Recovery Verified Through CFD Simulations, International Journal of Mechanical Engineering and Technology (IJMET), 14(6), 2023, pp. 23-36.

#### **Article Link:**

https://iaeme.com/MasterAdmin/Journal\_uploads/IJMET/VOLUME\_14\_ISSUE\_6/IJMET\_14\_06\_003.pdf

#### **Abstract Link:**

https://iaeme.com/Home/article\_id/IJMET\_14\_06\_003

**Copyright:** © 2023 Authors. This is an open-access article distributed under the terms of the Creative Commons Attribution License, which permits unrestricted use, distribution, and reproduction in any medium, provided the original author and source are credited.

This work is licensed under a Creative Commons Attribution 4.0 International License (CC BY 4.0).



☑ editor@iaeme.com